Ecotoxicology and Environmental Safety 175 (2019) 58–65

Contents lists available at ScienceDirect

Ecotoxicology and Environmental Safety

journal homepage: www.elsevier.com/locate/ecoenv

Mineral elements uptake and physiological response of *Amaranthus mangostanus* (L.) as affected by biochar

Weili Jia[a], Cuiping Wang[a,*], Chuanxin Ma[b,**], Jicheng Wang[a], Hongwen Sun[a], Baoshan Xing[c]

[a] Key Laboratory of Pollution Processes and Environmental Criteria, Ministry of Education, Tianjin Key Laboratory of Environmental Remediation and Pollution Control, College of Environmental Science and Engineering/Sino-Canada R&D Centre on Water and Environmental Safety, Nankai University, Tianjin 300071, China
[b] Department of Analytical Chemistry, The Connecticut Agricultural Experiment Station, New Haven, CT 06504, United States
[c] Stockbridge School of Agriculture, University of Massachusetts, Amherst, MA 01003, United States

ARTICLE INFO

Keywords:
Biochar
Amaranthus mangostanus
Mineral elements migration
Physiological response

ABSTRACT

Amaranthus mangostanus L. (amaranth) was hydroponically grown in different concentrations of biochar amended nutrient solution to investigate the mineral elements migration and physiological response of amaranth as affected by biochar. Our results showed that exposure to 26.6 g/L of biochar greatly increased the root and shoot K, Na and Al content, while 2.6 g/L of biochar greatly increased the root Ca and Mg content. The uptake of K and Al notably altered other elements' accumulation in shoots and roots upon the biochar exposure. The ratio of Ca: K in shoots and Mg: K in roots were negatively correlated to the biochar concentrations, while the ratio of Al: Ca and Al: Mg in roots were positively related to the biochar concentrations. The Al: Fe ratio was also polynomial correlated to the concentrations of biochar. The addition of biochar beyond 2.6 g/L resulted in the cell membrane and DNA damages in roots. The activity of SOD and CAT in 6.7 g/L biochar treated roots was significantly elevated as compared to the ones in other biochar treatments and was almost 2-fold of the control. The photosynthetic F_v/F_m intensity and subcellular structure in leaves were also compromised upon exposure to 26.6 g/L biochar. Taken together, biochar could significantly alter the mineral migration in amaranth and physiologically damage in the plants. It is essential to study the effect of biochar within appropriate concentrations on plants prior to wide application in agriculture.

1. Introduction

Biochar is the solid product from pyrolysis or “charring” of waste biomass residues of agricultural and forestry products (Sohi, 2012; Wang et al., 2010; Xu et al. 2013b, 2015), which has been considered great meaning when applied to soil on both agriculture and remediation (Tan et al., 2015; Zhang et al., 2013). For example, biochar alleviated salinity-caused growth depressions (Akhtar et al., 2015) and together with arbuscular mycorrhizal fungal inoculation resulted in an additional plant yield (Hammer et al., 2015). Typically, because most carbon in biochar has an aromatic structure and is very recalcitrant to enhance long-term carbon sequestration in the environment (Lehmann, 2007). Besides, compared with activated carbon, biochar appears to be a new potential low-cost and effective adsorbent (Tan et al., 2015) because of the abundant feedstocks (Xu et al., 2013a) and lower energy requirements in production process (Lu et al., 2012). In recent years, lots of studies have been devoted to investigate the application of biochar for pollutants removal from aqueous solution and soil. Therefore, biochar has been widely applied in the terrestrial environment, the influence of biochar on safety and quality of plants should arise our concerns.

A new paradigm suggested that biochar should be considered as the matrix for a new generation of mineral or organic slow-release fertilizers (Schmidt et al. 2015, 2017). Usually, biochar, as a nutrient source, directly controls plant root nutrient acquisition and indirectly alters soil nutrient content (Prendergast-Miller et al., 2014). Akhtar et al. (2015) reported that 5% (*w/w*) biochar addition reduced Na^+ concentration but increased K^+ concentration thus lowered Na^+/K^+ ratio in wheat leaf. Brantley et al. (2016) reported that biochar addition decreased ear-leaf Ca and Mn and exerted no main effect on ear-leaf N or Zn. However, studies on the migration of the released mineral elements from biochar in the exposure plant system and on their potential influence on plants are rather limited.

Biochar also affected the physiological properties of plants. For

* Corresponding author.
** Corresponding author.
E-mail addresses: wangcp@nankai.edu.cn (C. Wang), chuanxin.ma@ct.gov (C. Ma).

https://doi.org/10.1016/j.ecoenv.2019.03.039
Received 17 December 2018; Received in revised form 8 March 2019; Accepted 10 March 2019

example, in soil metal immobilization, biochar increased the soluble protein of Dwarf beans (Hmid et al., 2015). The crude protein composition could be affected by the combination of biochar and fertilizer treatments (Hossain et al., 2015). Biochar could significantly increased the leaf turnover and enhanced protein catabolism by increasing the leaf proteolytic activities (Noguera et al., 2012). As for biomass, the addition of biochar at approximate 30 t ha^{-1} was an appropriate rate for tomato production (Li et al., 2018). However, application of fash carbonization biochar negatively affected the corn biomass at the highest (4%) rate, probably because of the stress from high concentration of K luxury consumption pertaining to high ash and other toxic organic carbon (Butnan et al., 2015). Biochar application alters soil carbon (C) and nitrogen (N) dynamics (Clough et al., 2013), hence, it alters the C/N availability and the biological fixation of C/N ratio (Rondon et al., 2007). The ratio of C/N is one of the important indicators to evaluate plant growth and quality (Krapp et al., 2005; Royer et al., 2013). Therefore, biochar is very likely to influence the metabolism of plants via affecting C and N fixation, and a concentration-dependent experiment is desirable to understand the response of plant to biochar exposure.

Photosynthesis is another important parameter to evaluate the plant growth. When biochar was applied for red ferrosol, biochar altered a modest (but significant) improvement of the maximum electron transport rate and saturating photosynthetic rate (Xu et al., 2015). Besides, biochar application made up for the decrease of photosynthesis under different drought stress (Rizwan et al., 2018). Biochar could produce a widely influence on oxidative damage and antioxidant defense system of plants (Ashraf et al., 2015; Farhangi-Abriz and Torabian, 2017). Abbas et al. (2018) reported that biochar reduced the oxidative stress, increased the antioxidant enzyme SOD and CAT activity and decreased the POD activity in wheat under combined drought and Cd stress. Thus, it is important to evaluate the photosynthetic efficiency and oxidative stress induced physiological damages in plants.

In the present study, *Amaranthus mangostanus* (L.) (amaranth) was chosen to exposed to different concentration s of biochar. K, Na, Ca, Mg, Fe and Al were measured to clarify the fate of mineral elements (both nutrients and potentially toxic elements) in amaranth as affected by biochar. Physiological properties such as electrolytic leakage, soluble protein and C/N content were analyzed. In addition, the peroxidation damage such as MDA and γ-H2AX content, and activities of primary antioxidant enzyme such as SOD, CAT and POD were quantified. In order to evaluate the biochar effects on plants photosynthesis, we determined the chlorophyll content and chlorophyll fluorescence, including the maximum quantum efficiency of photosystem II (PSII) F_v/F_m and maximal electron-transport rate (ETR_{max}). At the cellular level, subcellular structure in leaves were observed. Our goal was to comprehensively understanding the amaranth defense and detoxification mechanisms, nutrient status and photosynthetic response in response to biochar exposure.

2. Materials and methods

2.1. Biochar characterization

The biochar was derived in furnace, increased the temperature at 10 °C/min to 400 °C, and kept for 5 h at 400 °C. Detailed information for biochar characterization was presented in our previous study (Jia et al., 2019). The content of available metals from the biochar was also determined according to National agricultural industry standards (NY/T 890-2004). Briefly, 5 g biochar was mixed with 10 mL of Diethylene triamine pentaacetic acid (DTPA) extract liquid. The mixture was shaken at 25 ± 2 °C for 2 h and filtered by a 0.45 μm filter membrane. The concentration of K, Na, Ca, Mg, Fe and Al was measured by an inductively coupled plasma mass spectroscopy (ICP-MS, Elan drc-e, Perkin Elmer, USA).

2.2. Experimental setup

Plant preparation. Amaranth seeds were surface-sterilized using 50% (*v/v*) ethanol for 15 min and then washed with deionized H_2O according to Ma et al. (2013) with mild modification. Briefly, sterilized amaranth seeds were germinated on moist filter paper and were germinated in half-strength Hoagland's solution in an environmentally controlled plant growth chamber (22 °C/18 °C; 14 h/8 h; day/night) (HH.BH-600, Tianjin Tianyu Experimental Equipment Co., Ltd, China) for 20 days. The uniform-sized amaranth seedlings (3 or 4 fully developed leaves) were then transferred into Hoagland's solutions and allowed to acclimatize for 5 days prior to biochar exposure.

Hydroponic system. Amaranth seedlings were grown in glass jars containing 180 mL full strength Hoagland's solution amended with different concentrations of powered biochar (1.3, 2.6, 6.7, 13.3 and 26.6 g/L biochar, 200–300 mesh size) for 10 days. The growth conditions were the same as mentioned above. Amaranth seedlings grown in Hoagland solution without addition of biochar were used as a control. Air was pumped into the growth media three times per day with 8 h interval to maintain the biochar suspension and to provide sufficient oxygen for roots. At harvest, biomass was measured across all treatments. Briefly, amaranth seedlings were washed with distilled water and dried prior to record the sample weight. A portion of fresh roots was used to analyze electrolytic leakage. The remaining shoots and roots were freeze-dried or stored at −80 °C freezer (DW-86L388A, Qingdao Haier Electric Appliance Co., Ltd., China) for further analysis. The growth media across all the treatments were also filtered and stored at −80 °C.

2.3. Elemental analysis

A portion of freeze-dried shoot and root samples were ground into fine powders and weighed into a closed Teflon vessel containing 6 mL of HNO_3 and 2.0 mL of H_2O_2. The mixture was digested at 140 °C for 7 min and then at 180 °C for 15 min in a microwave chemical reactor (MDS-86, Shanghai Sineo Microwave Chemical Technology Co., Ltd) according to Wang et al. (2017). The digests were finally diluted with deionized H_2O to a final volume of 25 mL. The content of K, Na, Ca, Mg, Fe and Al was measured using the same method as used in biochar mineral elements determination. An elemental analyzer (EA3000, Leeman Co., China) was used to measure the C and N content in amaranth roots and shoots.

2.4. Photosynthesis measurement and chloroplast structure observation

Photosynthesis analysis. Chlorophyll fluorescence, including the maximum quantum efficiency of photosystem II (PSII) F_v/F_m and maximal electron-transport rate (ETR_{max}) were measured using a IMAGING- PAM (Walz Ltd., Germany) according to Pfündel et al. (2008). The chlorophyll content was determined as described by Wang et al. (2014) and Arnon (1949). Detailed information for the sample preparation and analysis is given in the SI.

Chloroplast observation. The chloroplast structure was observed by a transmission electron microscopy (TEM; Hitachi H-7650, Hitachi Corp., Tokyo, Japan) at 180 KV (Nhan et al., 2015). Details for sample fixation and instrument parameters are provided in the SI.

2.5. Electrolytic leakage analysis

The electrolytic leakage (EL) of fresh roots was measured according to Wang et al. (2015) and Wei et al. (2007) with mild modification. Briefly, 0.1 g fresh amaranth root sections that 1.5–2 cm away from the root tip were rinsed thoroughly with deionized water to remove surface particles, then sectioned into 1 cm segments and placed in vials containing 10 mL distilled water. Samples were shaking at room temperature (25 °C) for 3 h. The electrical conductivity (EC) of the solution

(EC1) was measured after shaking using an electrical conductivity meter (XL200, Fisher accumet, America). Samples were subsequently placed in a thermostatic water bath at 100 °C for 15 min, and a second reading (EC2) was determined after the solutions were cooled to room temperature. Electrolytic leakage was calculated as EL = (EC1/EC2) × 100 and expressed as a percentage.

2.6. Roots oxidative damage assay

Malondialdehyde (MDA) content was measured using the thiobarbituric acid (TBA) test as described by Jambunathan (2010). Histones were isolated as described by Wu et al. (2011), and the level of H2AX phosphorylation (γ-H2AX) in the histone samples was analyzed using a plant γ-H2AX enzyme-linked immunosorbent assay (ELISA) kit (48 T, Hengyuan, Shanghai, China). Detailed information is given in the SI.

2.7. Soluble protein and antioxidant enzymes measurement

The protein content was measured by the Bradford method (Bradford, 1976). The antioxidant activities were measured according to Ma et al. (2016), detailed procedures are provided in the SI.

2.8. Data analysis

The values were averaged from three replicates and the error bars corresponded to standard error of the mean. A one-way analysis of variance (one-way ANOVA) followed by least significant difference (LSD) test was used to determine the statistical significance ($p \leq 0.05$) of each parameter among treatments performed on SPSS version 23.0. The detailed regression analysis by Origin 8.5 is provided in the SI.

3. Results and discussion

3.1. Nutrient uptake and migration in amaranth as affected by biochar

Previous studies have demonstrated that biochar could directly or indirectly affect the migration, transformation and phytoavailability of nutrients in soils (Alburquerque et al., 2014; Sun et al., 2016). The biochar used in our study consisted a high content of available K and Na (9597.5 and 1747.2 mg/kg, respectively). The content of essential macronutrient Mg and Ca was 144.7 and 556.8 mg/kg, respectively, and the content of micronutrient Fe was 159.9 mg/kg. In addition, the content of toxic Al was 325.2 mg/kg.

Due to the high content of K in biochar, the addition of all concentrations of biochar significantly increased the root and shoot K by 72.4–118.3% and 6.8–9.8% (except the shoot K at 2.6 g/L biochar), respectively (Fig. 1 A and B). The Ca content changed differently from K in amaranth, where 2.6 and 6.7 g/L biochar caused the root Ca content increased by 20.7 and 63.7% ($p \leq 0.05$) relative to the control (Fig. 1 C and D), respectively, while 26.6 g/L biochar significantly decreased the shoot Ca content by 18.9% compared to the control. The root Mg content was increased ($p \leq 0.05$) across all the biochar treatments as compared to the control; while only 2.6 and 6.7 g/L biochar notably elevated the shoot Mg content (Fig. 1 E and F). However, the variation of nutrient content in amaranth did not varied the fresh biomass of amaranth across all the biochar treatment (Figure S1A).

For micronutrients, both the root and shoot Na level were significantly increased by 45.5–112.7% and 109.2–371.2%, respectively (Fig. 1 G and H), as affected by 2.6–26.6 g/L biochar. Although the level of available Fe in biochar was 159.9 mg/kg, the addition of biochar markedly decreased the Fe content by 56.5–82.9% and 46.1–80.3% in roots and shoots, respectively (Fig. 1 I and J). In contrast, 13.3 and 26.6 g/L biochar increased Al content in root by 748.3–964.1%, and 2.6–26.6 g/L biochar increased shoot Al content by 132.3–218.2% (Fig. 1 K and L, $p \leq 0.05$). Biochar was rich in mineral elements, which affected nutrient uptake and migration in plants. However, not all the mineral elements content increased along with the biochar concentration increasing. This indicated potential interactions between elements might occurred upon the plant uptake, and only a suitable biochar concentration could give meaning to agricultural application. Therefore, the correlations between ratio of nutrient levels and biochar concentrations were analyzed as follows.

3.2. The correlation between nutrient levels and biochar concentrations in amaranth

Ratio of Ca: K, Mg: K, Fe: K, Al: Ca, Al: Mg and Al: Fe were calculated in different concentrations of biochar treated amaranth roots and shoots (Table 1). Significant decreases from 28.3 to 60.0% in Ca: K ratio in amaranth roots were found across all the biochar treatments, except 2.6 g/L, in which the Ca: K ratio had no change as compared to the control. However, in biochar treated shoots, only 26.6 g/L biochar significantly decreased the Ca: K ratio. Similarly, a decreasing trend in Mg: K ratio in biochar treated roots was evident, no significant change of Mg: K ratio was found in biochar treated shoots, except 6.7 g/L biochar, which significantly increased the Mg: K ratio. Interestingly, when adding biochar, the Fe: K ratio decreased significantly both in roots and shoots in relative to the control. The Al: Ca ratio in roots and shoots was approximately 8–12 and 3-fold of the respective control upon exposure to 13.3 and 26.6 g/L biochar, respectively. The Al: Mg ratio in roots and shoots was approximately 6–8 and 2-3 fold of the respective control upon exposure to 13.3 and 26.6 g/L biochar, respectively, and the Al: Fe ratio in roots and shoots was approximately 7–32 and 5-11 folds of the respective control upon exposure to 1.3–26.6 g/L biochar, respectively.

The correlation between nutrient ratios and biochar concentrations is shown in Fig. 2. A negative correlation between the Ca: K ratio and different concentrations of biochar was only found in shoots ($R^2 = 0.9028^{**}$) (Fig. 2A). Similar result was evident between the Mg: K ratio and different doses of biochar in roots ($R^2 = 0.6365^{*}$), but not in shoots (Fig. 2B). However, the Fe: K ratio was not correlated to the biochar concentrations (Data is not given). Therefore, with increasing the concentrations of biochar, the K accumulation in amaranth was elevated, but the Ca and Mg level were decreased. Rhodes et al. (2018) reported that the increase in the leaf K content led to decrease in leaf Ca and Mg content, suggesting that the presence of K within the certain level could interfere the bioavailability of Ca and Mg (Alam et al., 2003). Butnan et al. (2015) also found that the Ca: K and Mg: K ratio in corn significantly decreased with increasing the concentrations of biochar. Downregulations of the genes encoding the Mg transporters were found in pear leaf treated with 0.4 and 0.8 g/kg K via roots, demonstrating that K exhibited an antagonistic effect on the Mg uptake (Shen et al., 2019). Aligning with our findings, the high content of available K in biochar (9597.5 mg/kg) could cause the inhibition of Ca and Mg uptake by plant.

Regarding the correlation between the Al: Ca ratio and the biochar concentrations (Fig. 2C), the Al: Ca ratio in roots was positively correlated with biochar concentrations ($R^2 = 0.9502^{***}$). In Fig. 2D, the Al: Mg ratio in roots was also positively correlated with the biochar concentrations ($R^2 = 0.9552^{***}$). In Fig. 2 E, polynomial correlation between the Al: Fe ratio and different concentrations of biochar was evident ($R^2 = 0.9269^{**}$ in roots and $R^2 = 0.8158^{*}$ in shoots). These results suggested the excess accumulation of Al suppressed the Ca, Mg and Fe level in amaranth along with the biochar concentration increasing. The Al accumulation resulted in 61% and 72% reduction in the Ca and Mg content in maize, respectively (Mariano and Keltjens, 2005); exposure to 200 or 300 μm $AlCl_3$ significantly inhibited the Ca, Mg and Fe uptake by pineapple (Lin, 2010). One of the possible explanations could be that Al altered the membrane potential and the activity of ion channels and consequently caused the deficiency of Ca, Mg and Fe (Poschenrieder et al., 2008). The high accumulation of Al

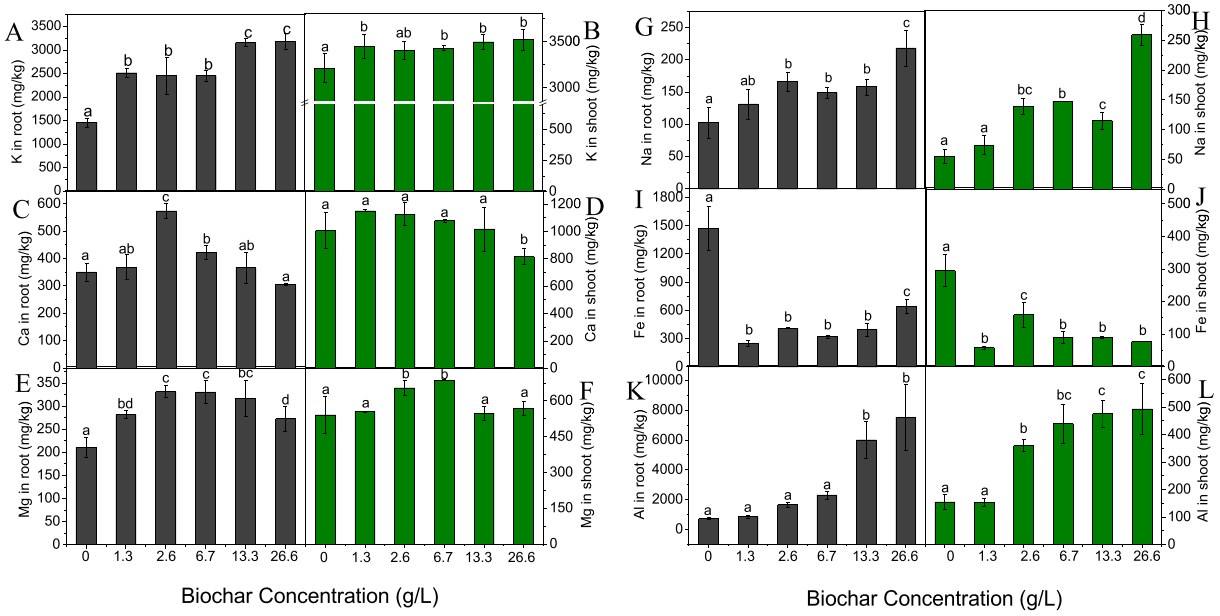

Fig. 1. The content of macroelements K in roots (A) and shoots (B), Ca in roots (C) and shoots (D), Mg in roots (E) and shoots (F); microelements Na in roots (G) and shoots (H), Fe in roots (I) and shoots (J); toxic Al in roots (K) and shoots (L) of amaranth exposed to different concentration of biochar. Data are mean ± standard error of three replicates. Values of each column followed by different letters indicate that the data points are significantly different at $p \leq 0.05$ (LSD's test).

Table 1
The ratio of Ca: K, Mg: K, Fe: K, Al: Ca, Al: Mg and Al: Fe in roots and shoots of amaranth as affected by different concentrations of biochar.

Ratio	Biochar concentration (g/L)					
	0	1.3	2.6	6.7	13.3	26.6
Ca: K in root	0.240d	0.146bc	0.235d	0.172c	0.116ab	0.096a
Ca: K in shoot	0.313b	0.334b	0.330b	0.315b	0.290b	0.232a
Mg: K in root	0.145d	0.112bc	0.134cd	0.135cd	0.100ab	0.085a
Mg: K in shoot	0.168ab	0.161a	0.192bc	0.200c	0.157a	0.161a
Fe: K in root	1.017b	0.100a	0.169a	0.130a	0.125a	0.201a
Fe: K in shoot	0.092c	0.017a	0.047b	0.026a	0.026a	0.022a
Al: Ca in root	2.04a	2.35a	2.85a	5.43a	16.9b	24.6b
Al: Ca in shoot	0.153a	0.133a	0.393b	0.440b	0.483b	0.443b
Al: Mg in root	3.39a	3.02a	4.94a	6.95a	18.82b	27.38c
Al: Mg in shoot	0.286a	0.276a	0.669b	0.692b	0.896c	0.634b
Al: Fe in root	0.482a	3.43b	4.00b	7.21c	15.24e	11.61d
Al: Fe in shoot	0.525a	2.64b	2.78b	5.44c	5.52c	4.69bc

Mean values with different letters are significantly different at $p \leq 0.05$ (LSD Test) among different biochar treatments in each row.

with biochar concentration increasing tend to antagonize Ca, Mg and Fe, and therefore significant correlations between Al: Ca, Al: Mg and Al: Fe ratio in amaranth root and biochar concentration were observed.

3.3. Physiological response of amaranth to biochar

Plant weight, electrolytic leakage, soluble protein and C:N ratio. Plant physiological responses are often the most visible evidence for amendment-induced abiotic stress in plants (Ma et al., 2018). Upon exposure to different concentrations of biochar, the electrolytic leakage in roots showed that biochar had no impact on ion leakage (Figure S1B), indicating the integrity of cell membrane. Compared to control, exposure to 13.3 and 26.6 g/L biochar significantly decreased the root soluble protein by 26.6 and 26.7%, respectively, and 26.6 g/L biochar decreased the shoot soluble protein by 25.4% significantly (Figure S1C and D). Plant soluble protein is one of the most activated proteins, including enzymes and metabolism modulators, which are sensitive to environmental stressors (e.g. drought, salt) (Chen et al., 2017; Yin et al., 2017). Therefore, the inhibition of soluble protein synthesis indicated that amaranth under high concentration of biochar induced stresses. The C: N ratio in both biochar treated roots and shoots suggested that the addition of different concentrations of biochar increased the C: N ratio but not obvious in general (Table S1). The changes in C: N ratio could alter plant nutrition and metabolisms, CO_2 and NH_4^+ are necessary in synthesizing glutamine (Zheng, 2009). Besides, C and N metabolisms are involved in almost all metabolic reactions. The N deficiency could decrease the C assimilation in leaves, and consequently impair the photosynthesis efficiency (Coruzzi and Bush, 2001; Coruzzi and Zhou, 2001). However, in the present study, the N decrease in shoot has no obvious effect on C accumulation in shoot. Therefore, biochar here caused minor effects on the plant nutrition and metabolisms via affecting C and N fixation.

Oxidative Damage in amaranth roots. The MDA formation is one of the most important indicators to represent whether the cell membrane is suffering oxidative damage. And H2AX phosphorylation (γ-H2AX) is a signal of DNA double strands break, an indicator of the DNA lesions (Jackson, 2002; Lang et al., 2012). Both the MDA and γ-H2AX content increasing could reflect oxidative stress occurs in plants. In amaranth roots, the MDA and γ-H2AX content increased by 43.1–76.1% and 58.9–90.9% in 2.6–26.6 g/L biochar treatments (Fig. 3A and B, $p \leq 0.05$), as compared to the control, respectively. To date, many studies have reported that biochar could alleviate the abiotic stressors induced oxidative damages in plants. For example, 10% and 20% (w/w, biochar/soil) biochar could potentially prevent bean seedlings from NaCl stress (Farhangi-Abriz and Torabian, 2017). Biochar at 10, 30 and 50 g/kg soil also lowered lipid peroxidation in leaves of *Ficus elastica* grown in Zn-contaminated soil (Kumar et al., 2018). However, in the present study, we found high concentration of biochar (above 2.6 g/L) caused oxidative damage to amaranth. Li et al. (2015) also found that with increasing the biochar concentrations from 4 to 8 g/beaker (4–8% biochar/soil), the malondialdehyde content in the tomato roots and leaves were increased, and the root cell necrosis was also evident.

Antioxidant enzyme activities in amaranth roots. Antioxidant enzymes, including SOD, CAT, and POD, are key scavengers for reactive oxygen species (ROS) (Alscher and Hess, 1993). Compared to control, exposure from 2.6 to 6.7 g/L biochar increased the root SOD activity from 39.2 to 58.8%, while 26.6 g/L biochar significantly decreased the SOD activity by 24.5% (Fig. 3C, $p \leq 0.05$). For CAT, biochar concentrations among

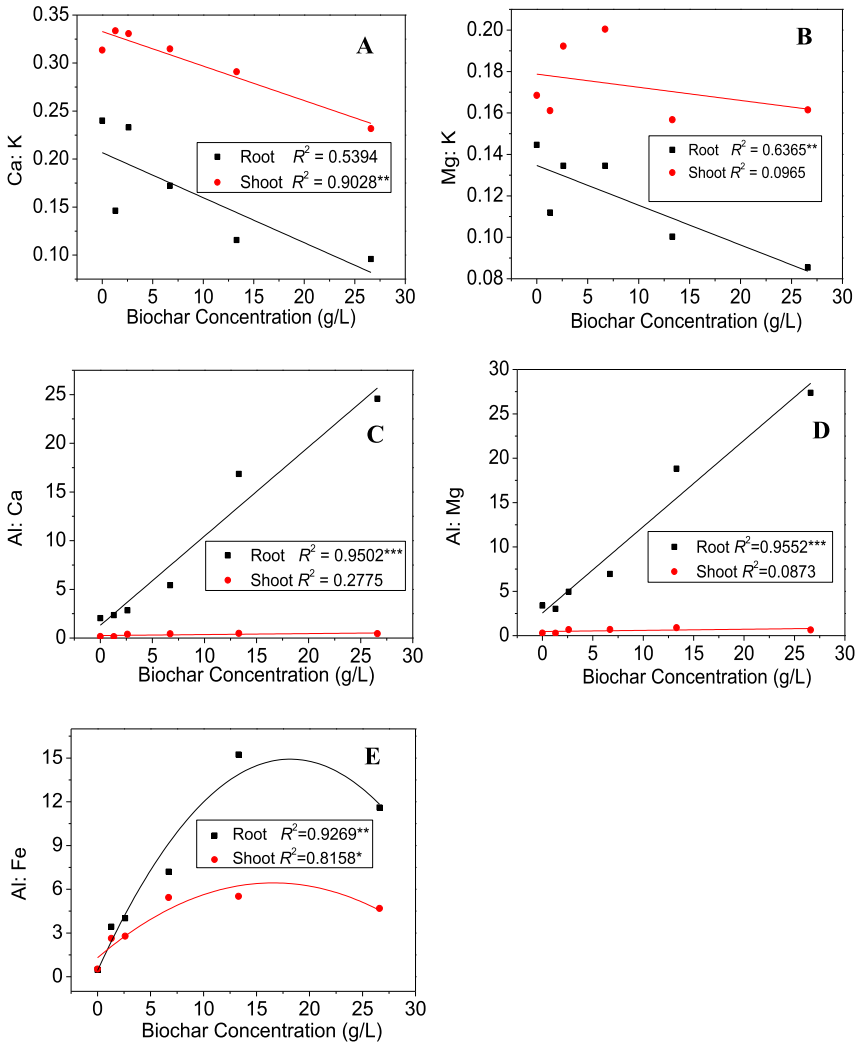

Fig. 2. The correlation between: Ca: K ratio in amaranth and biochar concentration (A); Mg: K ratio in amaranth and biochar concentration (B); Al: Ca ratio in amaranth and biochar concentration (C); Al: Mg ratio in amaranth and biochar concentration (D); Al: Fe ratio in amaranth and biochar concentration (E). (*$p \leq 0.05$, **$p \leq 0.01$, ***$p \leq 0.001$).

2.6–13.3 g/L obviously increased the CAT activity by 89.6–140.8%, while biochar concentrations among 1.3–26.6 g/L significantly increased the POD activity by 72.4–177.1%. In general, median concentration of biochar from 2.6 to 13.3 g/L biochar produced the most obvious effect on elevating antioxidant activities. Unexpectedly, 26.6 g/L biochar significantly decreased the activity of SOD, CAT and POD as compared to 6.7 g/L biochar. When the stress intensity exceeded the cells' endurance, the protein synthesis in cells could be inhibited, and

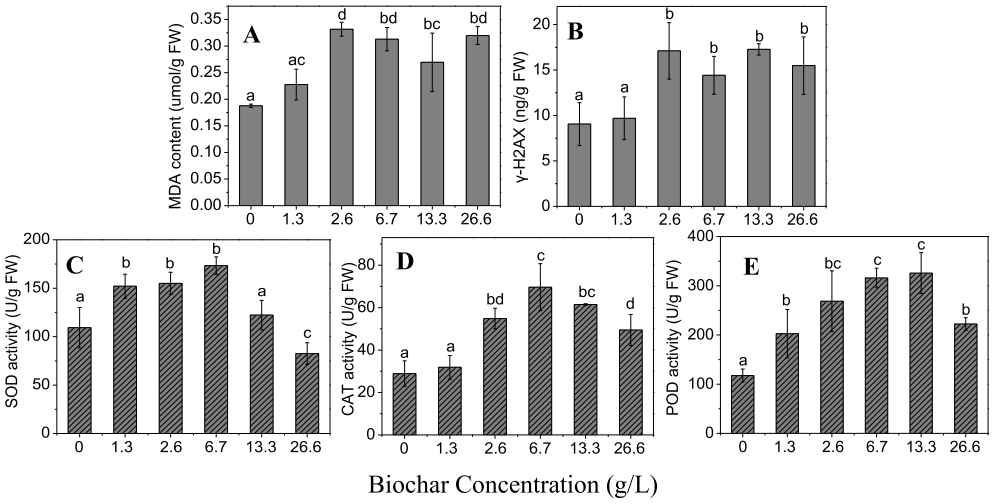

Fig. 3. Oxidative damage and antioxidant defense response. Figure A and B represent the content of MDA and γ-H2AX, Figure C–E represent the activity of SOD, CAT and POD in amaranth roots across all the treatments. Data are mean ± standard error of three replicates. Values of each column followed by different letters indicate that the data points are significantly different at $p \leq 0.05$ (LSD's test).

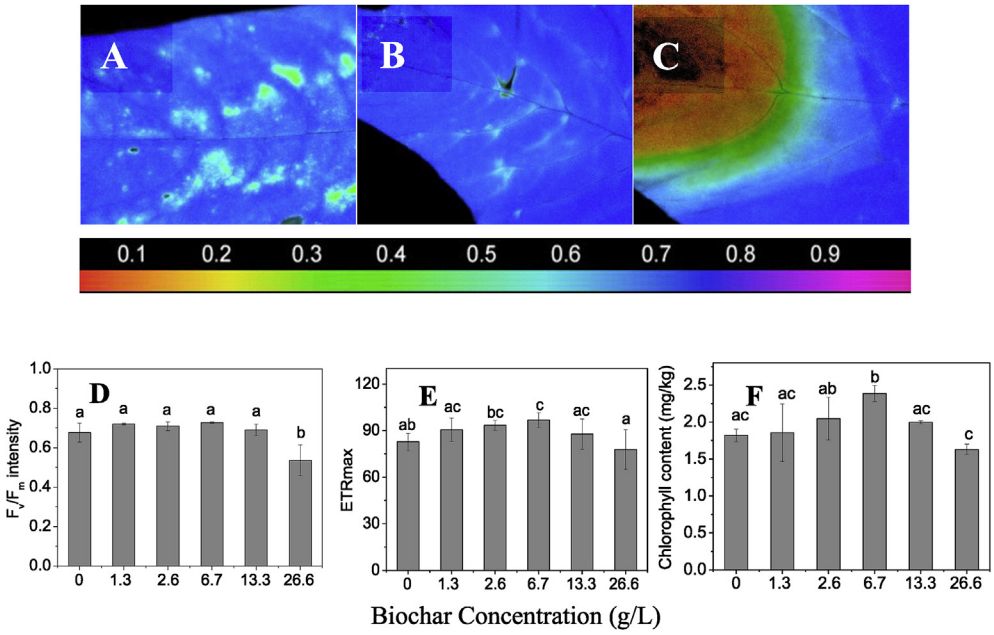

Fig. 4. Photosynthesis of amaranth treated with biochar. A-C are the images of F_v/F_m intensity in the treatment with control, 6.7 g/L biochar and 26.6 g/L biochar. Figure D–F represent the F_v/F_m intensity, ETR_{max} intensity and chlorophyll content across all the treatments. Data are mean ± standard error of three replicates (n = 3). Values followed by different word are significantly different at $p \leq 0.05$ (LSD's test).

subsequently suppress the activity of antioxidant enzymes (Lee and Lee, 2000). In the present study, the soluble protein content in roots and shoots at 26.6 g/L was significantly decreased by 35.4% and 24.7%, respectively, as compared to the one in the treatment with 6.7 g/L biochar (Figure S1C and 2D), indicating the presence of biochar could alter the protein synthesis.

3.4. Effects of biochar on photosynthetic system

Biochar is a potential amendment to improve plants' performance on photosynthesis (Xu et al., 2015). In the photochemical process, maximum quantum efficiency of photosystem II (PSII), F_v/F_m, represents the intrinsic efficiency of PSII. The decrease of F_v/F_m usually indicates the stress exposure of plants (Maxwell and Johnson, 2000). Electron-transport rate (ETR_{max}) reflects photosynthetic electron flow through PSI and PSII of plants. Therefore, F_v/F_m, ETR_{max} and the total chlorophyll content were measured to evaluate the effects of biochar on photosynthetic systems in amaranth. IMAGING-PAM allow us to visualize the F_v/F_m intensity and leaf morphology. Fig. 4A–C showed the images of the F_v/F_m intensity in amaranth leaves treated with control, 6.7 and 26.6 g/L biochar, respectively. When exposing to 26.6 g/L biochar, the F_v/F_m intensity decreased by approximately 20.7% (Fig. 4D, $p \leq 0.05$) in relative to control, suggesting high concentration of biochar could potentially compromise the photosynthetic systems. For ETR_{max}, no difference across all biochar treatments was found except 6.7 g/L biochar, where the ETR_{max} were minorly but significantly increased by 17.0% as compared to control (Fig. 4E). Similar to ETR_{max}, exposure to 6.7 g/L biochar elevated the chlorophyll content by 31.1%, and other treatments had no obvious impact as compared to the control (Fig. 4F). 1% Biochar could increase photosynthetic and accessory pigments (carotenoids, anthocyanin, and lycopene) by reducing cadmium uptake by tomato (Abid et al., 2017). Additionally, biochar that was equivalent to 2% organic carbon could also increase the chlorophyll content and the photosynthetic rate of maize by decreasing bioavailable Ni in the soil (Rehman et al., 2016). However, according to our present results, though 6.7 g/L biochar significantly enhanced the photosynthetic process, high concentration of biochar at 26.6 g/L hampered the photosynthesis in amaranth to some extent.

3.5. Effects of biochar on cellular structure

In the control (Fig. 5A), the plant cell is intact and the chloroplasts were in oval, where the internal stroma lamella was clearly observed (Fig. 5A and B). In the 6.7 g/L biochar treatment, no deformation of cell organelles was observed, the shape of the chloroplast is still as the same in the control (Fig. 5C and D). With the concentration increasing to 26.6 g/L, the chloroplasts became swollen and the pattern of the grana lamellae was irregular and blurring (Fig. 5E and F). In addition, starch granular formed in the stroma thylakoid. The salt stress induced by high concentration of biochar could be one of the possible reasons that imbalance the osmotic pressure and consequently compromise the chloroplast structure (Yu et al., 2010). This observation was also supported by the high levels of K, Na, and Al in shoots treated with 26.6 g/L biochar (Fig. 1B, H and L). Consequently, the photosynthetic efficiency was damaged as determined by F_v/F_m intensity.

4. Conclusions

Biochar has obvious effect on mineral uptake and migration in plants. 26.6 g/L biochar significantly increased K, Na and Al content in roots while 2.6 g/L biochar significantly enhanced Ca and Mg uptake in roots. Furtherly, Ca and Mg accumulation were influenced by K and Al uptake under the effect of biochar. The excessive biochar caused damage on the membrane and DNA in roots. 6.7 g/L biochar obviously elevated the activities of antioxidant enzyme in root and was almost 2-fold of the control. Finally, the photosynthesis and chloroplast structure were impaired upon exposure of 26.6 g/L biochar. Hence, comprehensively characterizing the biochar fate in plant system and considering the biochar concentrations will provide important information for biochar application in agriculture.

Acknowledgements

This work was supported by the Ministry of Science and Technology of China (2018YFC1802001), Natural Science Foundation of China (41673104), Tianjin Science and Technology Committee (17JCZDJC39600), Science and Technology Commission of Tianjin Binhai New Area (BHXQKJXM-PT-ZJSHJ-2017002), Fundamental Research Funds for the Central Universities, and 111 program, Ministry of Education of China (T2017002), and Tianjin Agricultrual Affair

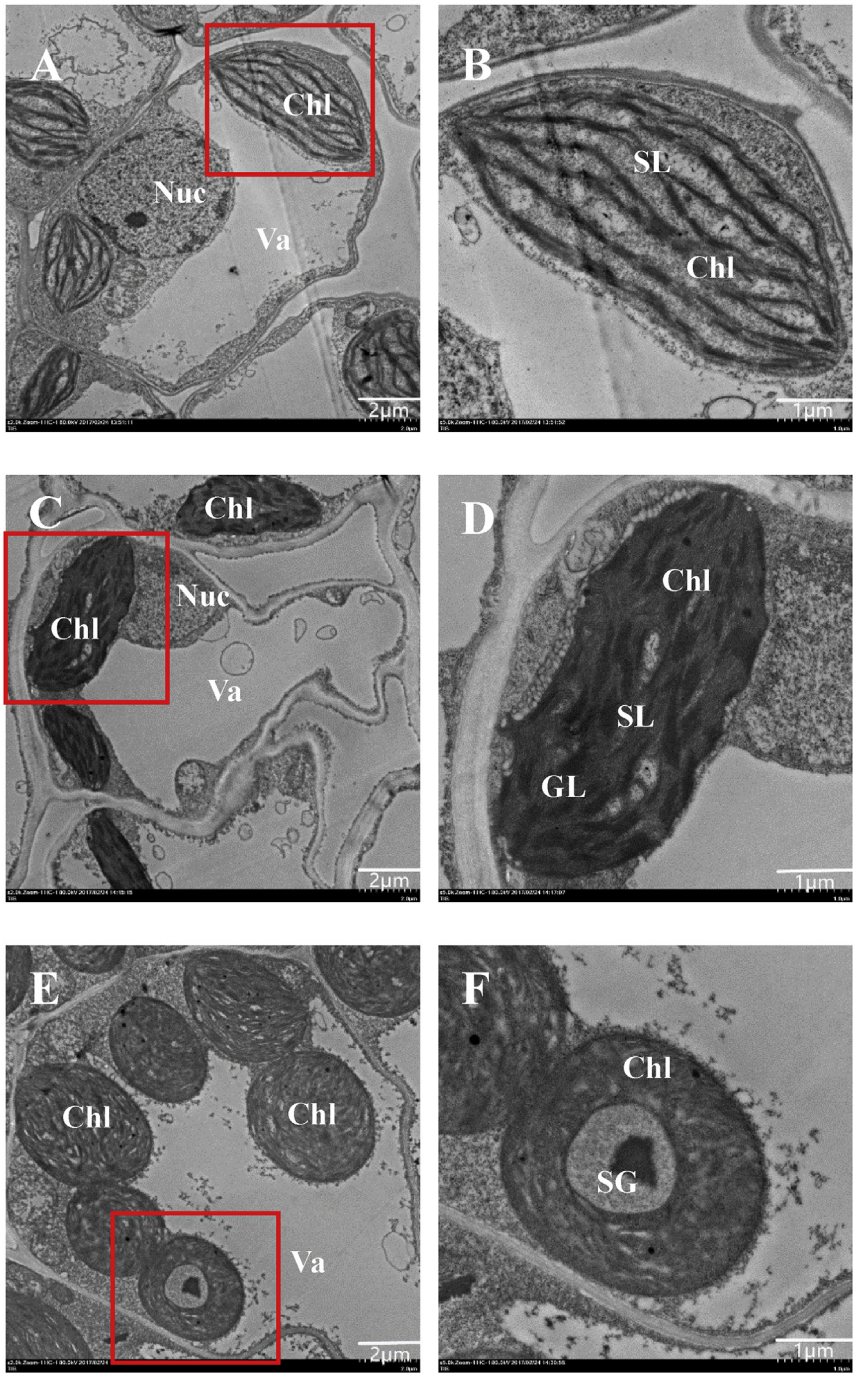

Fig. 5. TEM images of amaranth leaves as affected by different concentrations of biochar. Figure A, C and E represent the cellular structure of amaranth leaves upon exposure to control, 6.7 and 26.6 g/L biochar, respectively. Figure B, D and F represent the magnification of the red area of Figure A, B and C, respectively. Chl, chloroplast; Va, vacuole; Nuc: nucleus; GL: grana lamella; SL: stroma lamella; SG: starch grain. (For interpretation of the references to colour in this figure legend, the reader is referred to the Web version of this article.)

Committee, China (201604010).

Appendix A. Supplementary data

Supplementary data to this article can be found online at https://doi.org/10.1016/j.ecoenv.2019.03.039.

References

Abbas, T., Rizwan, M., Ali, S., et al., 2018. Biochar application increased the growth and yield and reduced cadmium in drought stressed wheat grown in an aged contaminated soil. Ecotoxicol. Environ. Saf. 148, 825–833. https://doi.org/10.1016/j.ecoenv.2017.11.063.

Abid, M., Danish, S., Zafar-ul-Hye, M., et al., 2017. Biochar increased photosynthetic and accessory pigments in tomato (Solanum lycopersicum L.) plants by reducing cadmium concentration under various irrigation waters. Environ. Sci. Pollut. Control Ser. 24 (27), 22111–22118.

Akhtar, S.S., Andersen, M.N., Liu, F., 2015. Residual effects of biochar on improving growth, physiology and yield of wheat under salt stress. Agric. Water Manag. 158, 61–68.

Alam, S., Kamei, S., Kawai, S., 2003. Amelioration of manganese toxicity in young rice seedlings with potassium. J. Plant Nutr. 26 (6), 1301–1314.

Alburquerque, J.A., Calero, J.M., Barrón, V., et al., 2014. Effects of biochars produced from different feedstocks on soil properties and sunflower growth. J. Plant Nutr. Soil Sci. 177 (1), 16–25.

Alscher, R.G., Hess, J.L., 1993. Antioxidants in Higher Plants.
Arnon, D.I., 1949. Copper enzymes in isolated chloroplasts. Polyphenoloxidase in Beta vulgaris. Plant Physiol. 24 (1), 1.
Ashraf, U., Kanu, A.S., Mo, Z., et al., 2015. Lead toxicity in rice: effects, mechanisms, and mitigation strategies—a mini review. Environ. Sci. Pollut. Control Ser. 22 (23), 18318–18332.
Bradford, M.M., 1976. A rapid and sensitive method for quantitation of micrograms quantities of protein utilizing the principle of protein-dye binding. Anal. Biochem. 72, 248–254.
Brantley, K., Savin, M., Brye, K., Longer, D., 2016. Nutrient availability and corn growth in a poultry litter biochar-amended loam soil in a greenhouse experiment. Soil Use Manag. 32 (3), 279–288.
Butnan, S., Deenik, J.L., Toomsan, B., Antal, M.J., Vityakon, P., 2015. Biochar characteristics and application rates affecting corn growth and properties of soils contrasting in texture and mineralogy. Geoderma 237, 105–116.
Chen, G., Fan, P., Feng, W., Guan, A., Lu, Y., Wan, Y., 2017. Effects of 5-aminolevulinic acid on nitrogen metabolism and ion distribution of watermelon seedlings under salt stress. Russ. J. Plant Physiol. 64 (1), 116–123.
Clough, T.J., Condron, L.M., Kammann, C., Müller, C., 2013. A review of biochar and soil nitrogen dynamics. Agronomy 3 (2), 275–293.
Coruzzi, G., Bush, D.R., 2001. Nitrogen and carbon nutrient and metabolite signaling in plants. Plant Physiol. 125 (1), 61–64.
Coruzzi, G.M., Zhou, L., 2001. Carbon and nitrogen sensing and signaling in plants: emerging 'matrixeffects'. Curr. Opin. Plant Biol. 4 (3), 247–253 [Review].
Farhangi-Abriz, S., Torabian, S., 2017. Antioxidant enzyme and osmotic adjustment changes in bean seedlings as affected by biochar under salt stress. Ecotoxicol. Environ. Saf. 137, 64–70.
Hammer, E.C., Forstreuter, M., Rillig, M.C., Kohler, J., 2015. Biochar increases arbuscular mycorrhizal plant growth enhancement and ameliorates salinity stress. Appl. Soil Ecol. 96, 114–121.
Hmid, A., Al Chami, Z., Sillen, W., De Vocht, A., Vangronsveld, J., 2015. Olive mill waste biochar: a promising soil amendment for metal immobilization in contaminated soils. Environ. Sci. Pollut. Res. Int. 22 (2), 1444–1456. https://doi.org/10.1007/s11356-014-3467-6.
Hossain, M.K., Strezov, V., McCormick, L., Nelson, P.F., 2015. Wastewater sludge and sludge biochar addition to soils for biomass production from Hyparrhenia hirta. Ecol. Eng. 82, 345–348. https://doi.org/10.1016/j.ecoleng.2015.05.014.
Jackson, S.P., 2002. Sensing and repairing DNA double-strand breaks. Carcinogenesis 23 (5), 687.
Jambunathan, N., 2010. Determination and Detection of Reactive Oxygen Species (ROS), Lipid Peroxidation, and Electrolyte Leakage in Plants Plant Stress Tolerance. Springer, pp. 291–297.
Jia, W., Ma, C., White, J.C., et al., 2019. Effects of biochar on 2, 2′, 4, 4′, 5, 5′-hexabrominated diphenyl ether (BDE-153) fate in Amaranthus mangostanus L.: accumulation, metabolite formation, and physiological response. Sci. Total Environ. 651, 1154–1165. https://doi.org/10.1016/j.scitotenv.2018.09.229.
Krapp, A., Saliba-Colombani, V., Daniel-Vedele, F., 2005. Analysis of C and N metabolisms and of C/N interactions using quantitative genetics. Photosynth. Res. 83 (2), 251–263.
Kumar, A., Tsechansky, L., Lew, B., Raveh, E., Frenkel, O., Graber, E.R., 2018. Biochar alleviates phytotoxicity in Ficus elastica grown in Zn-contaminated soil. Sci. Total Environ. 618, 188–198. https://doi.org/10.1016/j.scitotenv.2017.11.013.
Lang, J., Smetana, O., Sanchez-Calderon, L., et al., 2012. Plant Î³H2AX foci are required for proper DNA DSB repair responses and colocalize with E2F factors. New Phytol. 194 (2), 353–363.
Lee, D.H., Lee, C.B., 2000. Chilling stress-induced changes of antioxidant enzymes in the leaves of cucumber: in gel enzyme activity assays. Plant Sci. 159, 75–85.
Lehmann, J., 2007. A handful of carbon. Nature 447 (7141), 143–144.
Li, Y., Shen, F., Guo, H., et al., 2015. Phytotoxicity assessment on corn stover biochar, derived from fast pyrolysis, based on seed germination, early growth, and potential plant cell damage. Environ. Sci. Pollut. Control Ser. 22 (12), 9534–9543.
Li, C., Xiong, Y., Qu, Z., Xu, X., Huang, Q., Huang, G., 2018. Impact of biochar addition on soil properties and water-fertilizer productivity of tomato in semi-arid region of Inner Mongolia, China. Geoderma 331, 100–108. https://doi.org/10.1016/j.geoderma.2018.06.014.
Lin, Y., 2010. Effects of aluminum on root growth and absorption of nutrients by two pineapple cultivars [Ananas comosus(L.) Merr.]. Afr. J. Biotechnol. 9 (26), 4034–4041.
Lu, H., Zhang, W., Yang, Y., Huang, X., Wang, S., Qiu, R., 2012. Relative distribution of Pb2+ sorption mechanisms by sludge-derived biochar. Water Res. 46 (3), 854–862.
Ma, C., Chhikara, S., Xing, B., Musante, C., White, J.C., Dhankher, O.P., 2013. Physiological and molecular response of Arabidopsis thaliana (L.) to nanoparticle cerium and indium oxide exposure. ACS Sustain. Chem. Eng. 1 (7), 768–778.
Ma, C., Liu, H., Guo, H., et al., 2016. Defense mechanisms and nutrient displacement in Arabidopsis thaliana upon exposure to CeO 2 and in 2 O 3 nanoparticles. Environ. Sci.: Nano 3 (6), 1369–1379.
Ma, C., White, J.C., Zhao, J., Zhao, Q., Xing, B., 2018. Uptake of engineered nanoparticles by food crops: characterization, mechanisms, and implications. Ann. Rev. Food Sci.Technol. 9, 129–153. https://doi.org/10.1146/annurev-food-030117012657.
Mariano, E.D., Keltjens, W.G., 2005. Long-term effects of aluminum exposure on nutrient uptake by maize genotypes differing in aluminum resistance. J. Plant Nutr. 28 (2), 323–333. https://doi.org/10.1081/pln-200047625.
Maxwell, K., Johnson, G., 2000. Chlorophyll fluorescence–a practical guide. J. Exp. Bot. 51 (345), 659–668.
Nhan, L.V., Ma, C., Rui, Y., et al., 2015. Phytotoxic mechanism of nanoparticles: destruction of chloroplasts and vascular bundles and alteration of nutrient absorption. Sci. Rep. 5, 11618. https://doi.org/10.1038/srep11618.
Noguera, D., Barot, S., Laossi, K.R., Cardoso, J., Lavelle, P., Cruz de Carvalho, M.H., 2012. Biochar but not earthworms enhances rice growth through increased protein turnover. Soil Biol. Biochem. 52, 13–20. https://doi.org/10.1016/j.soilbio.2012.04.004.
Pfündel, E., Klughammer, C., Schreiber, U., 2008. Monitoring the effects of reduced PS II antenna size on quantum yields of photosystems I and II using the Dual-PAM-100 measuring system. PAM Appl. Notes 1, 21–24.
Poschenrieder, C., Gunse, B., Corrales, I., Barcelo, J., 2008. A glance into aluminum toxicity and resistance in plants. Sci. Total Environ. 400 (1–3), 356–368. https://doi.org/10.1016/j.scitotenv.2008.06.003.
Prendergast-Miller, M., Duvall, M., Sohi, S., 2014. Biochar–root interactions are mediated by biochar nutrient content and impacts on soil nutrient availability. Eur. J. Soil Sci. 65 (1), 173–185.
Rehman, M.Z., Rizwan, M., Ali, S., et al., 2016. Contrasting effects of biochar, compost and farm manure on alleviation of nickel toxicity in maize (Zea mays L.) in relation to plant growth, photosynthesis and metal uptake. Ecotoxicol. Environ. Saf. 133, 218–225. https://doi.org/10.1016/j.ecoenv.2016.07.023.
Rhodes, R., Miles, N., Hughes, J.C., 2018. Interactions between potassium, calcium and magnesium in sugarcane grown on two contrasting soils in South Africa. Field Crop. Res. 223, 1–11. https://doi.org/10.1016/j.fcr.2018.01.001.
Rizwan, M., Ali, S., Abbas, T., et al., 2018. Residual effects of biochar on growth, photosynthesis and cadmium uptake in rice (Oryza sativa L.) under Cd stress with different water conditions. J. Environ. Manag. 206, 676–683. https://doi.org/10.1016/j.jenvman.2017.10.035.
Rondon, M.A., Lehmann, J., Ramírez, J., Hurtado, M., 2007. Biological nitrogen fixation by common beans (Phaseolus vulgaris L.) increases with bio-char additions. Biol. Fertil. Soils 43 (6), 699–708.
Royer, M., Larbat, R., Bot, J.L., Adamowicz, S., Robin, C., 2013. Is the C:N ratio a reliable indicator of C allocation to primary and defence-related metabolisms in tomato? Phytochemistry 88 (2), 25–33.
Schmidt, H.P., Pandit, B.H., Martinsen, V., Cornelissen, G., Conte, P., Kammann, C.I., 2015. Fourfold increase in pumpkin yield in response to low-dosage root zone application of urine-enhanced biochar to a fertile tropical soil. Agriculture 5 (3), 723–741.
Schmidt, H.P., Pandit, B.H., Cornelissen, G., Kammann, C.I., 2017. Biochar-Based Fertilization with Liquid Nutrient Enrichment: 21 Field Trials Covering 13 Crop Species in Nepal. Land Degradation & Development.
Shen, C., Shi, X., Xie, C., et al., 2019. The change in microstructure of petioles and peduncles and transporter gene expression by potassium influences the distribution of nutrients and sugars in pear leaves and fruit. J. Plant Physiol. 232, 320–333. https://doi.org/10.1016/j.jplph.2018.11.025.
Sohi, S.P., 2012. Carbon storage with benefits. Science 338 (6110), 1034–1035.
Sun, J., He, F., Shao, H., Zhang, Z., Xu, G., 2016. Effects of biochar application on Suaeda salsa growth and saline soil properties. Environ.Earth Sci. 75 (8), 630.
Tan, X., Liu, Y., Zeng, G., et al., 2015. Application of biochar for the removal of pollutants from aqueous solutions. Chemosphere 125, 70–85.
Wang, H., Lin, K., Hou, Z., Richardson, B., Gan, J., 2010. Sorption of the herbicide terbuthylazine in two New Zealand forest soils amended with biosolids and biochars. J. Soils Sediments 10 (2), 283–289.
Wang, B., Wang, C., Li, J., Sun, H., Xu, Z., 2014. Remediation of alkaline soil with heavy metal contamination using tourmaline as a novel amendment. J. Environ. Chem. Eng. 2, 1281–1286. https://doi.org/10.1016/j.jece.2014.05.017.
Wang, S., Wang, Y., Luo, C., et al., 2015. Could uptake and acropetal translocation of PBDEs by corn be enhanced following Cu exposure? Evidence from a root damage experiment. Environ. Sci. Technol. 50 (2), 856–863.
Wang, C., Ma, C., Jia, W., Wang, D., Sun, H., Xing, B., 2017. Combined effects of dissolved humic acids and tourmaline on the accumulation of 2, 2', 4, 4', 5, 5'- hexabrominated diphenyl ether (BDE-153) in Lactuca sativa. Environ. Pollut. 231 (Pt 1), 68–77. https://doi.org/10.1016/j.envpol.2017.07.094.
Wei, L., Luo, C., Wang, C., Li, X., Shen, Z., 2007. Biodegradable chelating agent ethylenediaminedisuccinic acid reduces uptake of copper through alleviation of copper toxicity in hydroponically grown Chrysanthemum coronarium L. Environ. Toxicol. Chem. 26 (4), 749–754.
Wu, T., Li, X., Huang, H., Zhang, S., 2011. Enantioselective oxidative damage of chiral pesticide dichlorprop to maize. J. Agric. Food Chem. 59 (8), 4315–4320.
Xu, X., Cao, X., Zhao, L., 2013a. Comparison of rice husk-and dairy manure-derived biochars for simultaneously removing heavy metals from aqueous solutions: role of mineral components in biochars. Chemosphere 92 (8), 955–961.
Xu, X., Cao, X., Zhao, L., Wang, H., Yu, H., Gao, B., 2013b. Removal of Cu, Zn, and Cd from aqueous solutions by the dairy manure-derived biochar. Environ. Sci. Pollut. Control Ser. 20 (1), 358–368.
Xu, C.-Y., Hosseini-Bai, S., Hao, Y., et al., 2015. Effect of biochar amendment on yield and photosynthesis of peanut on two types of soils. Environ. Sci. Pollut. Control Ser. 22 (8), 6112–6125.
Yin, X., Cui, Y., Wang, M., Xia, X., 2017. Overexpression of a novel MYB-related transcription factor, OsMYBR1, confers improved drought tolerance and decreased ABA sensitivity in rice. Biochem. Biophys. Res. Commun. 490 (4), 1355–1361.
Yu, K., Meng, Q., Zou, J., 2010. Effects of Cd2+ on seedling growth, chlorophyll contents and ultrastructure in Maize. Acta Agric. Boreali Sin. 25 (3), 118–123.
Zhang, X., Wang, H., He, L., et al., 2013. Using biochar for remediation of soils contaminated with heavy metals and organic pollutants. Environ. Sci. Pollut. Control Ser. 20 (12), 8472–8483.
Zheng, Z.-L., 2009. Carbon and nitrogen nutrient balance signaling in plants. Plant Signal. Behav. 4 (7), 584–591.